Research Article

MOLECULAR PAIN

Molecular Pain
Volume 13: 1–12

DOI: 10.1177/1744806916688901
journals.sagepub.com/home/mpx

SAGE

Overexpression of suppressor of cytokine signaling 3 in dorsal root ganglion attenuates cancer-induced pain in rats

Jinrong Wei[1,*], Meng Li[1,*], Dieyu Wang[1], Hongyan Zhu[2], Xiangpeng Kong[1], Shusheng Wang[2], You-Lang Zhou[1], Zhong Ju[1], Guang-Yin Xu[1,2] and Guo-Qin Jiang[1]

Abstract

Background: Cancer-induced pain (CIP) is one of the most severe types of chronic pain with which clinical treatment remains challenging and the involved mechanisms are largely unknown. Suppressor of cytokine signaling 3 (SOCS3) is an important intracellular protein and provides a classical negative feedback loop, thus involving in a wide variety of processes including inflammation and nociception. However, the role of SOCS3 pathway in CIP is poorly understood. The present study was designed to investigate the role of SOCS3 in dorsal root ganglion (DRG) in the development of CIP.

Method: CIP was established by injection of Walker 256 mammary gland tumor cells into the rat tibia canal. Whole-cell patch clamping and Western blotting were performed.

Results: Following the development of bone cancer, SOCS3 expression was significantly downregulated in rat DRGs at L2–L5 segments. Overexpression of SOCS3, using lentiviral-mediated production of SOCS3 at spinal cord level, drastically attenuated mechanical allodynia and body weight-bearing difference, but not thermal hyperalgesia in bone cancer rats. In addition, overexpression of SOCS3 reversed the hyperexcitability of DRG neurons innervating the tibia, and reduced abnormal expression of toll-like receptors 4 in the DRGs.

Conclusions: These results suggest that SOCS3 might be a key molecular involved in the development of complicated cancer pain and that overexpression of SOCS3 might be an important strategy for treatment for mechanical allodynia associated with bone cancer.

Keywords

Cancer-induced pain, dorsal root ganglion, suppressor of cytokine signaling 3, toll-like receptors 4

Date received: 30 July 2016; revised: 21 October 2016; accepted: 22 November 2016

Introduction

Cancer-induced pain (CIP) resulting from primary tumors or tumors that metastasize to bone is one of the most severe and incapacitating types of chronic pain. Bone metastases had been identified at autopsy in up to 90% of patients who died from prostate cancer[1,2] and 85% of those who died from breast or lung cancer.[3,4] Like many chronic pain conditions, CIP becomes more severe with disease progression, almost half of cancer patients have inadequate or undermanaged pain control.[5,6] In aspect of the relative ineffectiveness and the adverse effects of the current available treatments, it is urgent to develop new potential therapeutic targets for cancer pain relief. However, mechanism underlying the

[1]Jiangsu Key Laboratory of Translational Research and Therapy for Neuro-Psycho-Diseases, Institute of Neuroscience, The Second Affiliated Hospital, Soochow University, Suzhou, P.R. China
[2]Center for Translational Medicine, Affiliated Zhangjiagang Hospital of Soochow University, Zhangjiagang, P.R. China

*Jinrong Wei and Meng Li contributed equally to this work.

Corresponding authors:
Guang-Yin Xu, Laboratory for Translational Pain Medicine, Institute of Neuroscience, Soochow University, 199 Ren-Ai Road, Suzhou 215123, P.R. China.
Email: guangyinxu@suda.edu.cn
Guo-Qin Jiang, Department of Surgery, The Second Affiliated Hospital of Soochow University, 1055 San-Xiang Road, Suzhou 215004, P.R. China.
Email: jiang_guoqin@163.com

development of CIP is not fully understood. Recent studies using rodent models of CIP suggested that sensitization of primary afferent neurons innervating tumor and the around tissues likely contributes to mechanical allodynia and thermal hyperalgesia.[7–9]

Suppressor of cytokine signaling 3 (SOCS3), induced by cytokine receptors, has been reported to act as feedback inhibitor of Janus kinase/signal transducer and activator of transcription 3 (JAK/STAT3) pathway, and thus negatively regulating signaling in numerous cell types.[10,11] The previous studies show that SOCS3 and its family members are potentially pivotal negative regulators of interleukin-6 (IL-6) signaling; with the stimulation of IL-6, SOCS3 works as a role in preventing IFN-gamma-like responses in cells.[12] SOCS3 has been reported to be involved in several inflammatory diseases, such as inflammatory arthritis,[13] intestinal inflammation,[14] and neuropathic pain.[15] Whether SOCS3 is involved in CIP remains unknown. Since the tumor-released products and tumor-induced injury to primary afferents can simultaneously drive the inflammation,[16,17] we hypothesize that SOCS3 signaling in dorsal root ganglion (DRG) may play an important role in the development of CIP.

Toll-like receptors (TLR4) are the cell surface proteins that participate in innate immune and endotoxin recognition,[18,19] and detect host cell's stress and damage that cause the release of host DNA, RNA, heat shock proteins, and cell membrane components.[20] TLR4-deficient mice have reduced bone destruction following mixed anaerobic infection.[21] Female rats with tibia tumors that displayed tactile allodynia and spontaneous pain are correlated with a significant increase in TLR4.[22] These data suggest that TLR4 is involved in CIP perception. Therefore, in this study, we tested the hypothesis whether SOCS3 played an important role in CIP and its possible interaction with TLR4 in DRG tissues of rats with bone cancer (BC). Using replication-deficient and self-inactivating lentiviral (LV) vectors,[23,24] we developed a feasible approach to induce SOCS3 overexpression in the DRG tissues. We showed that tumor cell injection significantly reduced the expression of SOCS3 in DRG tissues and that overexpression of SOCS3 attenuated the hyperalgesia, reversed the hyperexcitability of DRG neurons innervating the tibia, and reduced the expression of TLR4. Therefore, overexpression of SOCS3 might represent a novel strategy for BC pain therapy.

Materials and methods

Animals

Female Sprague-Dawley rats weighing 160–180 g were housed in temperature ($24 \pm 1^{\circ}C$) and light-controlled (12-h light/dark cycle) room with free access to standard rodent chow and water. Experiments were carried out in accord with protocols that were approved and monitored by the Institutional Animal Care and Use Committee at Soochow University and the Association of laboratory animals in Jiangsu Province, China.

Induction of CIP model

The procedures for induction of BC pain model were in accordance with the previous report.[25,26] In brief, rats were anesthetized with Chloral hydrate (360 mg/kg, i.p.) for surgery. A skin incision was made to expose the tibia plateau. A needle was then inserted into the medullary canal parallel to the tibia to create a pathway for the Walker 256 cell injection. Then, Walker 256 cells (4×10^5) or the same volume of normal saline (NS) (control group) was slowly injected into the tibia cavity by using a 10-μL microinjection syringe with 23-gauge needle. The syringe was left in place for an additional 2 min to avoid the tumor cells leaking out along the injection track.[27] All rats were allowed to recover from the surgery for at least three days prior to further experimentation.

Mechanical allodynia, thermal hyperalgesia, and weight-bearing experiments

The 50% paw withdrawal threshold (PWT) to a static mechanical stimulus was measured using von Frey filaments and the up-and-down methods, as described previously.[25] Rats ($n = 8$ in each group) were placed individually on an elevated iron mesh in a plastic cage, and they were allowed to adapt to the testing environment for 30 min. An ascending series of von Frey hairs (0.4, 0.6, 1.0, 1.4, 2.0, 4.0, 6.0, 8.0, 10.0, 15.0 g) were applied to stimulate the plantar aspect of each hind paw. A trial began with the application of the 2.0 g hair and with 15.0 g as the cutoff strength of von Frey filaments. A withdrawal of hind paw upon the stimulus was defined as a positive response. In the presence of a response, a filament of a greater force was applied. The tactile stimulus producing a 50% likelihood of withdrawal was determined by the "up-down" calculating method. The mean value was used as the force to produce withdrawal response.

The paw withdrawal latency (PWL) to radiant heat was also examined as described previously.[28,29] Rats were allowed to adapt to the acrylic enclosures on a transparent and clear glass plate for 30 min. A radiant heat source was focused on the plantar surface of the hindpaw. Measurements of PWL were taken by a timer that was started upon activation of heat source and stopped upon withdrawal of the hindpaw detected with a photodetector. A maximal cut-off time was set at 20 s

to prevent unnecessary tissue damage. Three measurements were taken for each rat. The averaged value was the result of each test session. The hindpaw was tested alternately with at least 5 min interval between consecutive tests.

Hind limb weight-bearing difference (WBD) was measured using a Dual Channel Weight Averager (Churchill Electronic Services Ltd). Rat was placed in a Perspex chamber designed so that each hindpaw rests on a separate transducer pad. The average was set to record the load on the transducer over 5 s and the two displayed readings represented the distribution of the rat's body weight on each paw. For each rat, the two numbers from each paw were taken and the results are presented as WBD.[30,31] All behavioral tests were carried out by a trained observer in a blinded manner.

LV vector production and intrathecal injection

The coding sequence of rat SOCS3, 5-ggtaagcctatccctaaccctctcctcggtctcgattctacg-3, was used for the experiment.[15] An additional scrambled sequence was also designed as a negative control (NC) (5′-ttctccgaacgtgtcacgtttc-3′). Replication-deficient, self-inactivating LV expressing vectors pFU-GW-RNAi-GFP [LV-SOCS3 and LV-NC] were generated. The cDNAs were subcloned into the vector (Shanghai Gene Chem Co, Ltd.). The resulting recombinant LV vectors were designated as LV-SOCS3 and LV-NC, respectively. As described previously, 293 T cells were co-transfected with 20 μg of pFU-GW-SOCS3 plasmid or pFU-GW-free and 15 μg of pHelper 1.0 and 10.0 μg of pHelper 2.0 packaging plasmids.[32] The culture medium was collected 48 h later, concentrated by ultracentrifugation, aliquoted. The final viral suspension was stored at −80°C until use. LV suspension was titrated and normalized for the p24 antigen (Beckman Coulter). The final titer of LV-SOCS3 and LV-NC were 1×10^9 TU/mL. A guiding needle (18G) was passed between the lumbar vertebrae 5 and 6 to enter the intrathecal space and 10 μL volume of lentivirus was slowly injected.

Western blotting analysis of SOSCS3 and TLR4 expression

The expressions of SOCS3 and TLR4 in L2-L5 DRGs from control rats and BC rats injected with LV-SOCS3 or LV-NC were measured using Western blotting analysis. Rats were rapidly sacrificed by cervical dislocation. L2-L5 DRGs were quickly dissected out and lysed, then lysates were left for 2 h to rotate at 4°C, and were then centrifuged at 12,000 r/min for 20 min at 4°C. Supernatants were collected and total protein concentration was titrated using a bicinchoninic acid (BCA) kit. Equivalent amounts of protein (20 μg) were fractionated on 10% polyacrylamide gels (Bio-Rad, California, USA). Then proteins were transferred to polyvinylidene-difluoride membranes (Bio-Rad) at 200 mA for 2 h. Membranes were blocked with 5% fat-free milk solution in Tris Buffered Saline (TBS) (50 mM Tris-HCl, 133 mM NaCl, pH = 7.4) for 1 h at room temperature and incubated overnight at 4°C with primary antibody (anti-SOCS3 at 1:500, Santa Cruz Biotechnology, Santa Cruz, California, USA or anti-TLR4 at 1:1000, Abcam, UK) in TBS containing 1% milk. After washed in TBST, membranes were then incubated with horseradish peroxidase-conjugated secondary antibodies (1:5000) in TBS containing 1% milk for 2 h at room temperature. Bands were revealed with an ECL kit (Amersham, Buckinghamshire, UK) and appropriate exposure to Kodak X-ray film. Membranes were subsequently stripped and re-probed for actin (anti-β-actin 1:4000, Chemicon, Temecula, California, USA). β-actins were used as a loading control. The densities of protein bands were analyzed using NIH image software. SOCS3 and TLR4 protein expressions were normalized to β-actin.

Retrograde labeling of DRG neurons innervating the tibia

To determine the origin of the primary afferent innervation of the tibia, 1, 19 -dioleyl-3, 3, 39, 3-tetramethylindocarbocyanine methanesulfonate (DiI, Invitrogen, Carlsbad, California) was used to retrogradely label the neurons, as described previously.[25] In brief, seven days after injection of tumor cells or NS, rats were anesthetized with chloral hydrate (360 mg/kg, intraperitoneal). A skin incision was made to expose the tibia plateau. A needle was then inserted into the medullary canal parallel to the tibia to create a pathway for the DiI injection. Then, a volume of 5 -μL DiI was slowly injected ipsilaterally to the tumor cell injected tibia cavity from the tibia plateau by a 10 -μL microinjection syringe with 23-gauge needle. The syringe was left in place for an additional 2 min to prevent the DiI from leaking out along the track. One week later, lumbar L2–L5 DRGs were dissected out to study its excitability by using patch clamp recordings or to perform immuno-fluorescent staining.

Dissociation of DRG neurons and patch clamping experiments

To isolate DRG neurons, rats (two weeks after injection of tumor cells or NS) were sacrificed by cervical dislocation, followed by decapitation, as described previously.[33] In brief, L2-L5 DRGs ipsilateral to the injection tibia were dissected out and transferred to an ice-cold, oxygenated fresh dissecting solution (in mM): 130 NaCl, 5 KCl, 1.5 $CaCl_2$, 2 KH_2PO4, 6 $MgSO_4$, 10 HEPES,

and 10 glucose. The pH of solution was adjusted to 7.2 and osmolarity was 305 mOsm. The DRGs were incubated in dissecting solution, which contained collagenase D (1.8 ~ 2.0 mg/ml; Roche, Indianapolis, IN) and trypsin (1.5 mg/ml; Sigma, St. Louis, MO), for 1.5 h at 34.5°C. DRGs were taken out, washed, and transferred to 2 mL of dissecting solution containing DNase (0.5 mg/ml; Sigma). Single cell suspension was subsequently obtained by repeated trituration through a series of flame-polished glass pipettes. Cells were then plated onto acid-cleaned glass coverslips. Coverslips containing adherent DRG cells were then put in a small recording chamber (0.5 mL) and attached to the stage of an inverting microscope (Olympus IX71, Tokyo, Japan), which is fitted with both fluorescent and phase objectives. DiI-labeled neurons were identified by their fluorescence. For patch clamp recordings, cells were perfused at room temperature with normal external solution. The external solution contains (in mM) 130 NaCl, 5 KCl, 2 KH_2PO4, 2.5 $CaCl_2$, 1 $MgCl_2$, 10 HEPES, and 10 glucose (pH = 7.2, adjusted with NaOH, osmolarity = 295–300 mOsm). Recording pipettes were pulled from borosilicate glass tubing using a horizontal puller (P-97, Sutter Instruments, California, USA) and typically had a resistance of 3.0 ~ 5.0 MΩ when filled with normal internal solution. Resting membrane potential (RP) and rheobase were recorded under current clamp configuration. Whole cell voltages, filtered at 2 ~ 5 kHz and sampled at 100 μs/point, were acquired with an EPC10 patch-clamp amplifier and stored on a computer using FitMaster (HEKA, Germany). All experiments were performed at room temperature (22 ~ 24°C).

Immunofluorescence study of SOCS3 and TLR4

One week after DiI injection, rats were perfused transcardially with 300 mL phosphate-buffered saline (PBS) followed by 300 mL ice-cold 4% paraformaldehyde in PBS. L2-L5 DRGs were removed and postfixed for 4 h in paraformaldehyde and cryoprotected overnight in 20% sucrose in PBS. For triple labeling, 10 μm sections of DRG were simultaneously incubated with SOCS3 (1:200), TLR4 (1:200), CD11b (1:200), β-tubulin (1:500), and GFAP (1:1000) antibodies for overnight at 4°C and then incubated with secondary antibody with Alexa Fluor 488 and 355 for 2 h at room temperature. NC was performed by omitting primary antibodies. Sections were viewed with filter cubes appropriate for DiI (rhodamine filter), Alexa 355, and 488. Images were captured and analyzed using Metaview software.

Data analysis

Data are expressed as mean ± SEM for electrophysiology, behavior, and molecular assays. Statistical analyses were conducted using OriginPro 8 (OriginLab, US) and SPSS statistics 17.0 software and were performed by Student's t-test for two-sample data and by Mann–Whitney test following Friedman ANOVA or Kruskal–Wallis ANOVA followed by Tukey's post hoc test for multiple comparisons where appropriate. Normality was verified for all data before analyses. A p value < 0.05 was set as the level of statistical significance.

Results

Tumor cell injection produced pain hypersensitivity

To confirm cancer development in the tibia, we examined the bone with an X-ray machine and anatomic studies 14 days after injection of tumor cells (4×10^5) or NS into tibias. As shown in the radiographic images, the tibia bone matrix and the cortex were normal in the NS injection group (CON, Figure 1(a), left). However, in tumor cell injection group, the bone showed signs of absorbance of bone tissue and erosion of the cortical bone in the proximal epiphysis close to the site of the injection (BC, Figure 1(a), right). Anatomic study showed that 14 days after injection of Walker 256 tumor cells, the proximal epiphysis of the tumor cells bearing tibia was destroyed (BC, Figure 1(b), right) while no damage was observed in NS injection group (CON, Figure 1(b), left). Importantly, rats treated with Walker 256 tumor cells displayed a gradual increase in sensitivity to von Frey filament stimulation. The PWT to von Frey filaments in the tumor-bearing hind paw of rats decreased from the baseline level 13.10 ± 1.40 g to 3.57 ± 0.49 g and 3.25 ± 0.49 g, 14 and 21 days after injection, respectively (Figure 1(c), ***$p < 0.001$; $n = 8$ rats for each group, Mann–Whitney test following Friedman ANOVA). Similarly, the PWL to the radiant heat stimulation began to decrease at day 14 and maintained at day 21 after injection (Figure 1(d)). The mean PWL was 14.23 ± 0.20 s prior to implantation of tumor cells. The mean PWL was 6.51 ± 0.16 s and 6.33 ± 0.13 s at day 14 and 21 after tumor cell injection, respectively (Figure 1(d), ***$p < 0.001$, $n = 8$ rats for each group, Mann–Whitney test following Friedman ANOVA). However, there was no obvious difference in the PWT or PWL between the control rats and the contralateral side of tumor-injected rats (Figure 1(e) and (f), $p > 0.05$, $n = 8$ rats for each group, Mann–Whitney test following Friedman ANOVA). In addition, the hind limb WBD was also examined. Rats injected with Walker 256 tumor cells showed a significant increase in hind limb WBD beginning from day 14 and lasting for one week within our observation time period (Figure 1(g)). The WBD was 2.70 ± 2.79 g before tumor cell injection and increased to 54.32 ± 2.10 g at day 14 and 62.75 ± 5.15 g at day 21 (Figure 1(g), ***$p < 0.001$, $n = 6$ rats for each

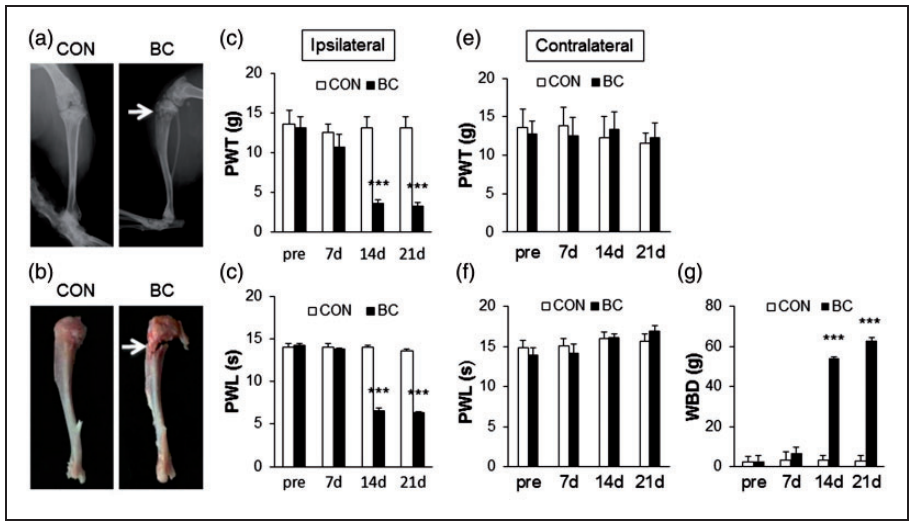

Figure 1. Injection of tumor cells induced bone destruction and developed pain hypersensitivity. (a) Radiographic images (a, left) and anatomic study (b, left) showed no damage of the tibia bone matrix and the cortex in control group. However, the tumor cells bearing tibia showed signs of absorbance of bone tissue and erosion of the cortical bone in the proximal epiphysis (a, right) and anatomic study showed the proximal epiphysis of the tumor cells bearing tibia was destroyed (b, right) at 14 days post injection. (c) The mechanical PWT was decreased significantly on the ipsilateral side in BC group at 14 and 21 days after surgery compared to the control group (***$p < 0.001$, $n = 8$ for each group, Mann–Whitney test following Friedman ANOVA). (d) The PWL to heat was decreased significantly on the ipsilateral side in BC group at 14 and 21 days after surgery compared with the control group (***$p < 0.001$, $n = 8$ for each group, Mann–Whitney test following Friedman ANOVA). (e, f) There was no obvious difference in the PWT and PWL between the control rats and the contralateral side of tumor-injected rats ($p > 0.05$, $n = 8$ for each group, Mann–Whitney test following Friedman ANOVA). (g) In BC group, the body WBD was dramatically increased between two hind limbs at 14 and 21 days after surgery when compared with the control group (***$p < 0.001$, $n = 6$ for each group, Mann–Whitney test following Friedman ANOVA).

group, Mann–Whitney test following Friedman ANOVA). In contrast, the NS-injected rats (CON) had no significant alteration in PWT (Figure 1(c)), PWL (Figure 1(d)), or WBD (Figure 1(g)) during the time course of post-injection. These data suggest that injection of Walker 256 tumor cells into the tibial canal resulted in CIP in rats.

Tumor cell injection led to downregulation of SOCS3 expression in Ipsilateral DRGs

Interestingly, tumor cell injection significantly reduced the expression of suppressor of cytokine signaling-3 (SOCS3) at the protein levels in ipsilateral L2-L5 DRGs when compared with NS-injected group (Figure 2(a)). The relative densitometry of SOCS3 was 0.08 ± 0.01 in the control group (CON) and 0.02 ± 0.01 in the BC group (Figure 2(a), **$p < 0.01$, $n = 4$ rats for each group, student's t-test). However, SOCS3 protein levels were not altered in contralateral L2-5 and ipsilateral T7-10 DRGs of the same tumor-injected rats. The relative densitometry of SOCS3 in contralateral L2-5 DRGs was 0.40 ± 0.13 in BC group and 0.53 ± 0.04 in CON group (Figure 2(b), $p > 0.05$, $n = 4$ rats for each group, student's t-test). The relative densitometry of SOCS3 in ipsilateral T7-10 DRGs was 0.65 ± 0.01 in the BC group and 0.46 ± 0.03 in CON group (Figure 2(c), $p > 0.05$, $n = 4$ rats for each group, student's t-test). These data suggest that the tumor-injection effects were local in special DRGs and in the injected side.

Since DRG tissues consist of many kinds of cells, immunohistochemical staining of β-tubulin, CD11b, and GFAP with SOCS3 were performed in the present study. Figure 3 showed that SOCS3 were co-localized with some of β-tubulin (top) positive DRG neurons but not with CD11b positive microglia cells (middle) and GFAP positive astrocytes (bottom). To evaluate the specificity of the SOCS3 primary antibody, we performed additional experiments by adding SOCS3 pre-absorption antigen. After SOCS3 antibody was pre-absorpted, DRG neurons were not stained (Figure 3, bottom right).

Overexpression of SOCS3 by LV infection attenuated pain hypersensitivity of BC rats

To increase the protein level of SOCS3 in DRGs, we developed a highly efficient method of LV-mediated delivery of SOCS3 cDNA for overexpression as described previously.[15] NC lentivirus (LV-NC, 10 μl) was used as controls. After intrathecal injection of LV-SOCS3 (10 μl), the expression of SOCS3 at protein level was enhanced in BC rats. The relative densitometry

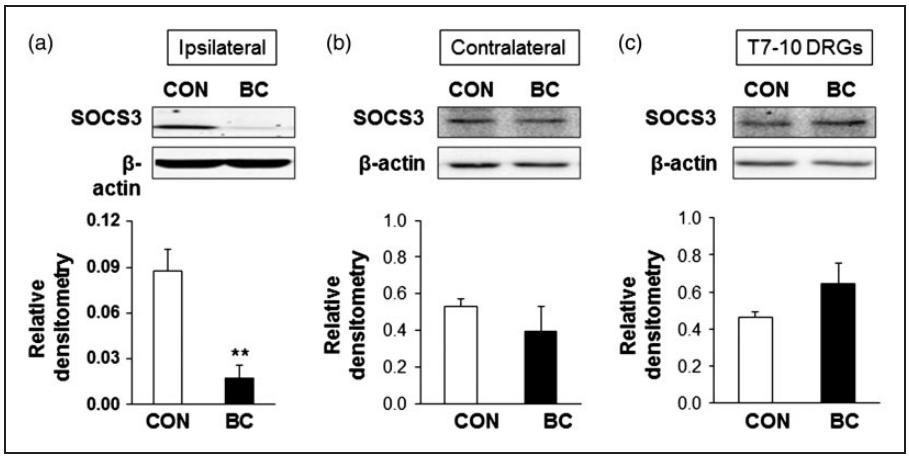

Figure 2. SOCS3 protein level was decreased in DRGs in BC rats. (a) Compared with the control group, SOCS3 protein level was greatly decreased in ipsilateral L2–L5 DRGs of BC rats, $^{**}p < 0.01$, $n = 4$ for both groups, student's t-test. (b) SOCS3 protein level was not changed in contralateral L2–L5 DRGs ($p > 0.05$, $n = 4$, student's t-test). (c) SOCS3 protein level was not altered in ipsilateral T7-10 DRGs ($p > 0.05$, $n = 4$, student's t-test).

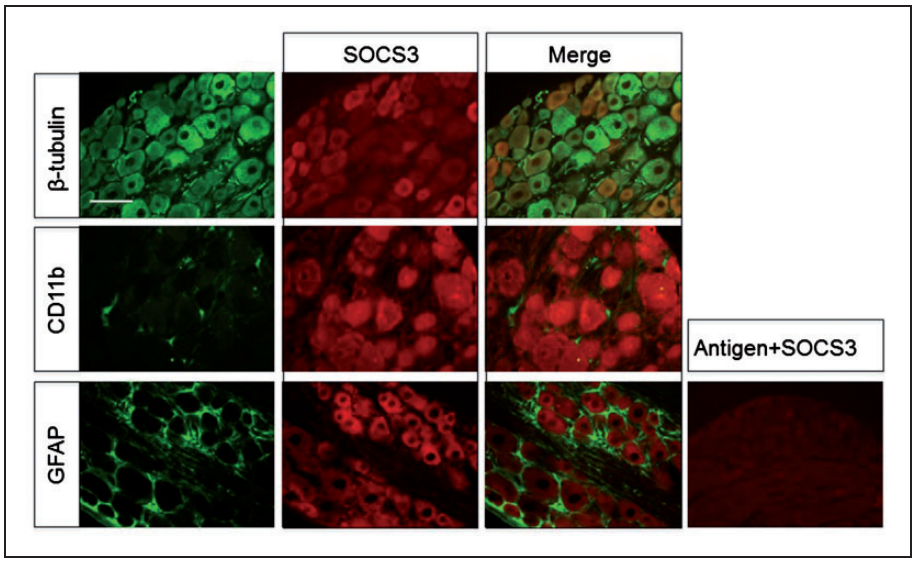

Figure 3. Immunohistochemical staining of β-tubulin, CD11b, and GFAP with SOCS3 in DRGs. SOCS3 were co-localized with some of β-tubulin (top) positive DRG neurons but not with CD11b positive microglia cells (middle) and GFAP positive astrocytes (bottom). After SOCS3 antibody was pre-absorpted, DRG neurons were not stained (bottom right). Bar = 50 μm.

was 0.06 ± 0.00 in the LV-SOCS3 group and 0.03 ± 0.01 in the LV-NC group (Figure 4(a), $^{*}p < 0.05$, compared with LV-NC, student's t-test, $n = 4$ rats for each group). Importantly, intrathecal injection of LV-SOCS3 produced a strong antinociceptive effect in BC rats. The decreased PWTs were partially reversed after LV-SOCS3 injection when compared with LV-NC injection in BC rats (Figure 4(b), $^{*}p < 0.05$, $n = 8$ rats for each group, Mann-Whitney test following Friedman ANOVA). Further, rats injected with LV-SOCS3 showed a significant reduction in hind limb body WBD at day 14 and day 21 when compared with the LV-NC groups (Figure 4(d), $^{***}p < 0.001$, $n = 8$ for each group, Mann–Whitney test following Friedman ANOVA). However, thermal hyperalgesia induced by tumor cells were not alleviated by intrathecal injection of LV-SOCS3 (Figure 4(c), $n = 8$ rats for each group, Mann–Whitney test following Friedman ANOVA).

Overexpression of SOCS3 reversed hyperexcitability of DRG neurons innervating the tibia of CIP rats

Next, we investigated whether overexpression of SOCS3 changed electrophysiological properties of DRG neurons

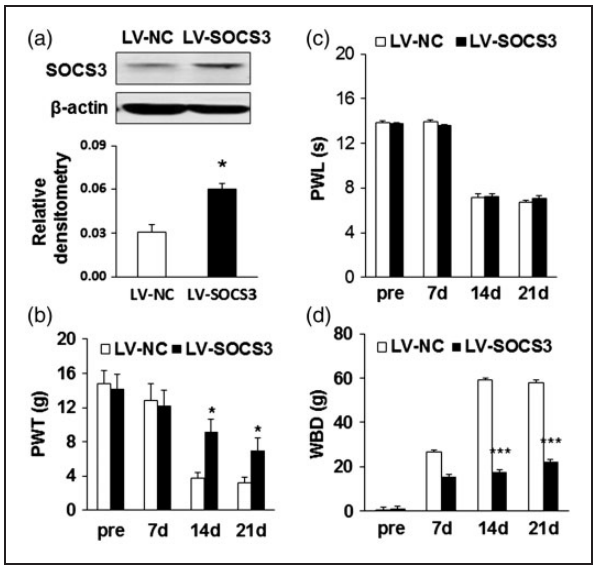

Figure 4. Injection of LV-SOCS3 enhanced expression of SOCS3 and relieves CIP. (a) Intrathecal injection of LV-SOCS3 at 10 μl significantly increased the SOCS3 protein level in L2–L5 DRGs in BC rats when compared with LV-NC injected BC rats (*$p < 0.05$, $n = 4$ for each group, Student's t-test). (b) The mechanical PWT was increased significantly on the ipsilateral side in LV-SOCS3 group at 14 and 21 days after surgery when compared with the LV-NC group (*$p < 0.05$, $n = 8$ for each group, Mann–Whitney test following Friedman ANOVA). (d) The PWL to heat was not altered significantly on the ipsilateral side in LV-SOCS3 group at 14 and 21 days after surgery compared with the LV-NC group ($n = 8$ for each group). (e) In LV-SOCS3 group, the body BWD was dramatically decreased at 14 and 21 days after surgery when compared with the NC (***$p < 0.001$, $n = 6$ for each group, Mann–Whitney test following Friedman ANOVA).

innervating the tibia. Acutely isolated tibia innervating DRG neurons (Figure 5(a)) were labeled by DiI (Figure 5(c)) and GFP (Figure 5(b)), which were overexpressed with SOCS3 or LV-NC. The RP of the DiI-labeled neurons from rats injected with tumor cells showed a slight but significant depolarization. Overexpression of SOCS3 significantly hyperpolarized RP (Figure 5(d), ***$p < 0.001$, compared with CON, $n = 14$ neurons from CON and $n = 24$ neurons from LV-NC, Kruskal–Wallis ANOVA followed by Tukey's post hoc test; ###$p < 0.001$, compared with LV-NC, $n = 12$ neurons from LV-SOCS3). The rheobase was significantly reduced after tumor cell injection while it was increased after LV-SOCS3 injection intrathecally (Figure 5(e), ***$p < 0.001$, LV-NC vs. CON, $n = 14$ neurons for CON and $n = 24$ neurons for LV-NC; ###$p < 0.001$, compared with LV-NC, $n = 12$ neurons for LV-SOCS3, Kruskal–Wallis ANOVA followed by Tukey's post hoc test). The action potential (AP) threshold was hyperpolarized after tumor cell injection while it was depolarized after LV-SOCS3 injection intrathecally (Figure 5(f), ***$p < 0.001$, LV-NC vs. CON, $n = 14$ neurons for CON and $n = 24$ neurons for LV-NC; ##$p < 0.01$, compared with LV-NC, $n = 12$ neurons for LV-SOCS3, Kruskal–Wallis ANOVA followed by Tukey's post hoc test).

In addition, representative traces of APs evoked by 1000 ms depolarizing ramp current injection at 100 pA (left), 300 pA (middle), and 500 pA (right) of DRG neurons from control, LV-NC, and LV-SOCS3 group of rats under current-clamp conditions were shown in Figure 6. Tumor cell injection remarkably increased the number of APs in response to a 100 pA, 300 pA, and 500 pA ramp current stimulation when compared with control rats (Figure 6, *$p < 0.05$, **$p < 0.01$, ***$p < 0.001$, LV-NC vs. CON, $n = 14$ neurons for CON and $n = 24$ neurons for LV-NC, Kruskal–Wallis ANOVA followed by Tukey's post hoc test). Overexpression of SOCS3 greatly reduced the number of APs evoked by 100 pA (Figure 6(d)), 300 pA (Figure 6(e)), and 500 pA (Figure 6(f)) ramp current stimulation (Figure 6, #$p < 0.05$, compared with LV-NC, $n = 24$ neurons for LV-NC and $n = 14$ neurons for LV-SOCS3, Kruskal–Wallis ANOVA followed by Tukey's post hoc test). These findings demonstrated that CIP elevated the excitability of tibia-specific lumbar DRG neurons and that overexpression of SOCS3 reversed the hyperexcitability of these neurons.

Overexpression of SOCS3 reversed the upregulation of TLR4 in DRGs of BC rats

We then examined the role of TLR4 in CIP since these receptors have been reported to be involved in development of inflammatory pain[34] and visceral pain hypersensitivity.[35] The protein level of TLR4 was slightly but significantly increased in L2-5 DRGs of BC rats when compared with control rats. The relative densitometry was 0.41 ± 0.08 ($n = 4$) and 0.70 ± 0.06 ($n = 4$) for control and BC rats, respectively (Figure 7(a), *$p < 0.05$, student's t-test), indicating tumor cell injection promoted expression of TLR4 in DRGs. We next determined the expression of TLR4 after LV-SOCS3 injection. Interestingly, overexpression of SOCS3 significantly reduced the expression of TLR4. The relative densitometry of TLR4 was 0.53 ± 0.06 ($n = 4$) and 0.37 ± 0.03 ($n = 4$) for LV-NC and LV-SOCS3, respectively (Figure 7(b), *$p < 0.05$, student's t-test). Further experiment showed that TLR4 were co-expressed with SOCS3 in DRG neurons innervating the tibia (Figure 7(c)). As mentioned previously, tibia innervating DRG neurons were labeled by DiI in red in Figure 7(c) (top left, arrows). SOCS3 positive DRG neurons were displayed in blue in Figure 6(c) (top middle, arrows). TLR4 receptor positive DRG neurons were displayed in green in Figure 6(c) (top right, arrows). Merge of double labeling

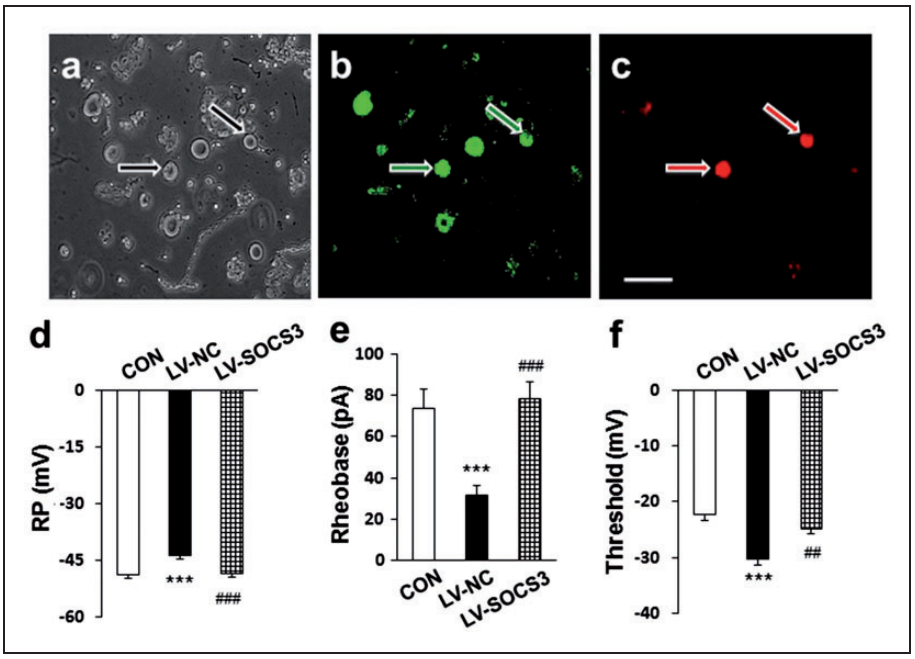

Figure 5. Treatment with LV-SOCS3 reduced the hyperexcitability of tibia-specific lumbar DRG neurons. (a) Images of acutely dissociated DRG neurons. (b) Some of the same DRG neurons in (a) were labeled by GFP, which overexpressed SOCS3 or LV-NC. (c) Two of the same DRG neurons in (a) were labeled by DiI (red). Arrows indicate that these neurons were GFP and DiI double-labeled neurons. Bar = 50 μm. (d) RP was depolarized after tumor cell injection (BC) and was hyperpolarized after LV-SOCS3 treatment. (e) The rheobase was reduced after tumor cell injection and was increased after LV-SOCS3 injection. (f) AP threshold was hyperpolarized after tumor cell injection and was depolarized after LV-SOCS3 injection. n = 14 neurons from 4 control rats; n = 24 neurons from 4 LV-NC rats; n = 14 neurons from 4 LV-SOCS3 rats, ***$p < 0.001$, LV-NC versus control; ##$p < 0.01$, ###$p < 0.001$, LV-SOCS3 versus LV-NC, Kruskal–Wallis ANOVA followed by Tukey's post hoc test.

of DiI and SOCS3 in DRGs was shown in Figure 7(c) (bottom left, arrows). Merge of TLR4-positive staining and DiI labeling was shown in Figure 7(c) (bottom middle, arrows). Merge of SOCS3 staining and TLR4 receptors labeling was shown in Figure 7(c) (bottom right, arrows).

Discussion

The present study demonstrated that injection of Walker 256 tumor cells into rat tibia resulted in the reduction of SOCS3 expression in DRGs of rats accompanied by prolonged mechanical allodynia and thermal hyperalgesia, and an enhanced body WBD. Further observation showed that overexpression of SOCS3 by LV strategy significantly attenuated the mechanical hyperalgesia in rats with BC. Although reasons for the difference were unknown, it is likely that SOCS3 can regulate downstream signal molecules responsive to mechanical stimulus rather than those to thermal stimulus. It is thought that thermal algesia is mostly mediated by TRPV1[12,36] and that mechanical algesia is likely mediated by mechanically gated channels such as the degenerin (DEG/ENaC) family and acid-sensing ion channel 2.[37] Future investigation into the mechanisms underlying the difference is definitely warranted. Nevertheless, it is of interest to target SOCS3 as an important molecule for treatment for mechanical allodynia of cancer pain.

In accord with the behavior changes, DRG neurons innervating the tibia showed a parallel alteration. Tumor cell injection enhanced the neuronal hyperexcitability while overexpression of SOCS3 reverses the hyperexcitability of DRG neurons. The primary afferent neurons with their cell bodies located in DRGs play an important role in detecting and conducting the peripheral stimulation or sensation, thus activation of DRG neurons leads to pain hypersensitivity.[38,39] In the present study, inhibition of neuronal excitability by overexpression of SOCS3 might help us to understand the antinociceptive effect of overexpression of SOCS3. Future experiments are needed to investigate how SOCS3 signaling modulates DRG neuronal excitability. Since patch clamp experiments were performed on GFP and DiI double-labeled DRG neurons, this enables us to make sure that neurons recorded in the present study were tibia innervating and SOCS3 overexpression neurons. Although LV infected different size neurons (Figure 4(b)), the DiI labeled neurons are mainly small and medium size neurons (Figure 4(c)), suggesting that the recorded neurons are pain related. Of note is that the control RPs

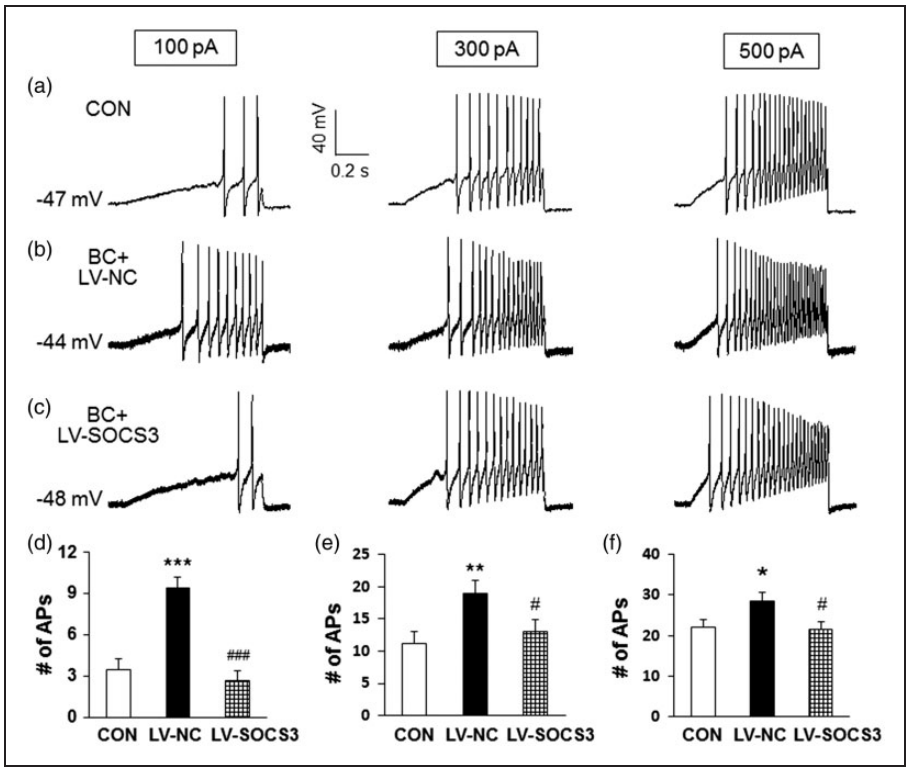

Figure 6. Overexpression of SOCS3 reduced the cell firing frequency. (a–c) Representative traces of APs induced by 1000 ms depolarizing current injection at 100 pA (left), 300 pA (middle), and 500 pA (right) ramp stimulation in DRG neurons from CON (a) and LV-NC (b), and LV-SOCS3 (c) rats. Numbers in the left side of each trace are the RPs of each neuron recorded. Tumor cells injection resulted in a significant increase in the number of APs induced by 100 pA (a), 300 pA (b), and 500 pA (c) ramp current stimulation of DRG neurons when compared with control neurons. LV-SOCS3 overexpression decreased the number of APs induced by a 100 pA, 300 pA, and 500 pA ramp current stimulation when compared with LV-NC, respectively. (d–f) Bar graphs showing the average number of APs elicited by 100 pA, 300 pA, and 500 pA ramp current stimulation in CON and BC rats injected with LV-NC or LV-SOCS3 (*$p < 0.05$, **$p < 0.01$, ***$p < 0.001$, LV-NC vs. CON; #$p < 0.05$, ###$p < 0.001$, LV-SOCS3 vs. LV-NC, Kruskal–Wallis ANOVA followed by Tukey's post hoc test).

(about −50 mV) look a little bit shallow compared with the reported values.[40] We do not know the exact reasons, but it is likely that the intrinsic features of L2 ~ L5 DRG neurons are different from those reported from other DRG neurons. Another possibility is that injection of DiI and overexpression of LV-NC might have impacted potassium/sodium pump activity and relative permeability, thus affecting the RP. In our previously published paper, we showed that P2X3 receptors are sensitized in pain hypersensitivity under BC conditions.[25] It is likely that purinergic receptors might be involved in mechanical pain hypersensitivity. Future experiments are needed to determine the roles of other ion channels such as TRPV1 and TRPA1.

The mechanism underling negative regulation of SOCS3 in pain hypersensitivity is largely unknown. SOCS3 was expressed in neurons and microglia in the spinal cord,[41] hypothalamic neurons,[42] astrocytes of the rat Hippocampus,[43] and retinal ganglion cells of zebra fish.[44] SOCS3 modulation has previously been implicated in anti-hyperalgesia in various models of neuropathic pain. Previous studies suggested that SOCS3 might interact with IL-6 and JAK2-STAT3.[45,46] However, whether SOCS3 was expressed in primary afferent neurons is unknown. We showed in the present study that SOCS3 was not only expressed in DRG neurons but also co-expressed with TLR4 positive DRG neurons innervating the tibia. However, it is not co-expressed with CD11b, a marker for microglial cells and GFAP, a marker for astrocytes. It has been reported that TLR4 level was increased in the spinal cord in rats with BC-induced pain and that its level was gradually increased with the bone destruction and the progress of BC pain.[22,47] In addition, the TLR4 antagonist relieved the cancer pain,[48] indicating a role of TLR4 in cancer pain. In the present study, the expression of TLR4 were increased in DRGs of rats with cancer pain but were decreased after SOCS3 overexpression. These data support our hypothesis that SOCS3-induced antinociceptive role might be mediated by inhibition of TLR4 expression in DRG neurons. Although the detailed mechanisms for the regulation of TLR4 by SOCS3 require to be further

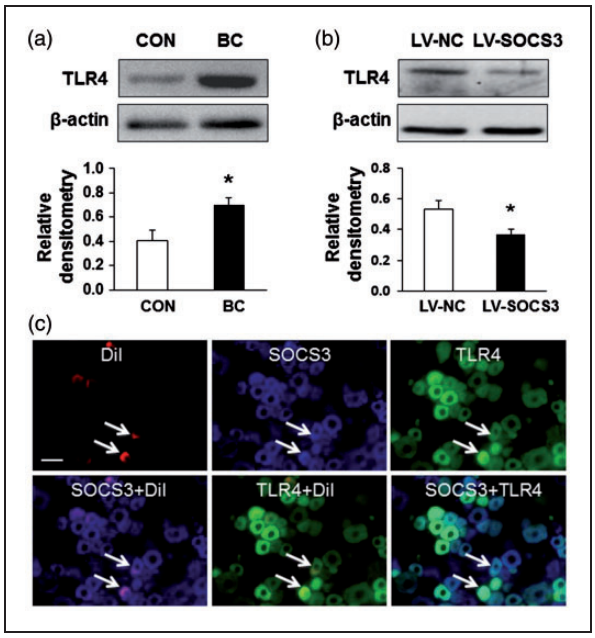

Figure 7. Overexpression of SOCS3 reversed the increase of TLR4 expression. (a) Western blots and bar graph showed the mean density relative to β-actin for TLR4 receptors from BC rats was significantly increased when compared with controls (CON; *$p < 0.05$; $n = 4$ for each group, student's t-test). (b) After LV-SOCS3 treatment, the relative TLR4 receptors density was decreased when compared with LV-NC group (*$p < 0.05$; $n = 4$ for each group, student's t-test). (c) Co-expression of SOCS3 with TLR4 receptors in tibia innervating DRG neurons. L5 DRG cells innervating the tibia were labeled with DiI in red (top left, arrows). SOCS3 positive cells are shown in blue (top middle). TLR4 receptors positive cells are shown in green (top right). Bar in the top left of figure (c) equals 50 μm.

studied, we showed for the first time that TLR4 might be one of downstream targets for SOCS3 under cancer pain conditions. The molecular mechanisms underlying the signaling pathway of SOCS3-meidated suppression of TLR4 remains largely unknown. Host SOCS3 regulates the innate immune response by controlling and limiting the proinflammatory response through negative feedback inhibition of cytokine receptors.[49] One candidate cell surface molecule for inducing proinflammatory cytokines is TLR4, which initiates a signal transduction pathway after binding to a ligand that ultimately results in NF-kB activation.[50,51] SOCS3 is composed of a kinase inhibitory region, a classical srchomology 2 (SH2) domain, and a SOCS box. The SOCS box is conserved in all cytokine-inducible SH2-domain-containing protein-SOCS family proteins.[49] One function of the SOCS box is to recruit components of the ubiquitin-transferase system and to coordinate their assembly and ability to ubiquitinylate target proteins.[52] TRAF6 protein is also likely a target for SOCS3 proteins.[53,54] Other mechanisms such as transforming growth factor beta signaling, immune receptors,[54,55] and JAK2/STAT3 signaling pathway[56,57] might be also participated.

In summary, tumor cell injection led to downregulation of SOCS3 expression in DRG neurons, which was negatively correlated with enhanced neuronal excitability, TLR4 upregulation, and pain hypersensitivity. Overexpression of SOCS3 attenuated pain hypersensitivity, reversed the excitability, and reduced the expression of TLR4 in DRGs of BC rats. Our data suggest that modulating SOCS3 expression might represent a novel strategy for treatment for cancer pain hypersensitivity.

What's already known about this topic?

SOCS3 is an important intracellular protein and provides a classical negative feedback loop, thus involving in a wide variety of processes including inflammation and nociception. However, the role of SOCS3 pathway in CIP remains poorly understood.

What does this study add?

Overexpression of SOCS3 using LV-mediated techniques significantly attenuated the mechanical pain hypersensitivity and reversed the hyperexcitability of DRG neurons innervating the tibia of rats.

Author contributions

JRW researched and analyzed data and wrote the manuscript. ML researched and analyzed data, prepared figures. DYW researched data. HYZ researched data. XK researched data. SSW analyzed data. Y-LZ researched and analyzed data. ZJ analyzed data. G-QJ analyzed data and wrote the manuscript. G-YX designed and supervised the experiments, and edited the manuscript. All authors discussed the results and commented on the manuscript. JW and ML contributed to this work equally.

Declaration of Conflicting Interests

The author(s) declared no potential conflicts of interest with respect to the research, authorship, and/or publication of this article.

Funding

The author(s) disclosed receipt of the following financial support for the research, authorship, and/or publication of this article: This work was supported by grants from National Natural Science Foundation of China (81070884 and 81471137 to GYX, 81401796 to YLZ) and from the Priority Academic Program Development of Jiangsu Higher Education Institutions of China. This project is subject to the second affiliated hospital of Soochow university preponderant clinic discipline group project funding (XKQ2015008).

References

1. Rana A, Chisholm GD, Khan M, et al. Conservative management with symptomatic treatment and delayed hormonal manipulation is justified in men with locally advanced carninoma of the prostate. *BJU* 1994; 74: 637–641.
2. Bowen C, Bubendorf L, Voeller HJ, et al. Loss of NKX3.1 expression in human prostate cancers correlates with tumor progression. *Cancer Res* 2000; 60: 6111–6115.
3. Harssema H. Field measurements of odorous air pollution with panels. In: Nielsen VC, Voorburg JH and L'Hermite P (eds) *Odour and ammonia emissions from livestock farming*. London: Elsevier Appl. Sci. Publ., 1991, pp.203–211.
4. Popat K, Mcqueen K and Feeley TW. The global burden of cancer. *Best Pract Res Clin Anaesthesiol* 2013; 27: 399–408.
5. Mercadante S. Malignant bone pain: pathophysiology and treatment. *Pain* 1997; 69: 1–18.
6. De Wit R, Van, Dam F, Loonstra S, et al. The Amsterdam Pain Management Index compared to eight frequently used outcome measures to evaluate the adequacy of pain treatment in cancer patients with chronic pain. *Pain* 2001; 91: 339–349.
7. Ye Y, Dang D, Viet CT, et al. Analgesia targeting IB4-positive neurons in cancer-induced mechanical hypersensitivity. *J Pain* 2012; 13: 524–531.
8. Zheng Q, Fang D, Liu MJ, et al. Suppression of KCNQ/M (Kv7) potassium channels in dorsal root ganglion neurons contributes to the development of bone cancer pain in a rat model. *Pain* 2013; 154: 434–448.
9. Zhou S, Fei D and Gu X. Non-coding RNAs as Emerging Regulators of Neural Injury Responses and Regeneration. *Neurosci Bull* 2016; 32: 1–12.
10. Larsen L and Röpke C. Suppressors of cytokine signalling: SOCS. *Acta Pathol Microbiol Immunol Scand* 2002; 110: 833–844.
11. Trengove MC and Ward AC. SOCS proteins in development and disease. *Am J Clin Exp Immunol* 2013; 2: 1–29.
12. Julius D and Basbaum AI. Molecular mechanisms of nociception. *Nature* 2001; 413: 203–210.
13. Liu X, Croker BA, Campbell IK, et al. Key role of suppressor of cytokine signaling 3 in regulating gp130 cytokine-induced signaling and limiting chondrocyte responses during murine inflammatory arthritis. *Arthritis Rheumatol* 2014; 66: 2391–2402.
14. Suzuki A, Hanada T, Mitsuyama K, et al. CIS3/SOCS3/SSI3 plays a negative regulatory role in STAT3 activation and intestinal inflammation. *J Exp Med* 2001; 193: 471–481.
15. Dominguez E, Mauborgne A, Mallet J, et al. SOCS3-mediated blockade of JAK/STAT3 signaling pathway reveals its major contribution to spinal cord neuroinflammation and mechanical allodynia after peripheral nerve injury. *J Neurosc* 2010; 30: 5754–5766.
16. Raghavendra V, Tanga F and Deleo JA. Inhibition of microglial activation attenuates the development but not existing hypersensitivity in a rat model of neuropathy. *J Pharm Exp Ther* 2003; 306: 624–630.
17. Luger NM, Honore P, Sabino MA, et al. Osteoprotegerin diminishes advanced bone cancer pain. *Cancer Res* 2001; 61: 4038–4047.
18. Kumar H, Kawai T and Akira S. Pathogen recognition in the innate immune response. *Biochem J* 2009; 420: 1–16.
19. Li C, Yan Y, Cheng J, et al. Toll-like receptor 4 deficiency causes reduced exploratory behavior in mice under approach-avoidance conflict. *Neurosci Bull* 2016; 32: 127–136.
20. Miyake K. Innate immune sensing of pathogens and danger signals by cell surface Toll-like receptors. *Semin Immunol* 2007; 19: 3–10.
21. Hou L, Sasaki H and Stashenko P. Toll-like receptor 4-deficient mice have reduced bone destruction following mixed anaerobic infection. *Infect Immun* 2000; 68: 4681–4687.
22. Liu SL, Yang JP, Wang LN, et al. Down-regulation of toll-like receptor 4 gene expression by short interfering RNA attenuates bone cancer pain in a rat model. *Mol Pain* 2010; 6: 1197–1198.
23. Meunier A, Mauborgne A, Masson J, et al. Lentiviral-mediated targeted transgene expression in dorsal spinal cord glia: tool for the study of glial cell implication in mechanisms underlying chronic pain development. *J Neurosci Methods* 2008; 167: 148–159.
24. Eleftheriadou I and Mazarakis ND. Lentiviral vectors for gene delivery to the nervous system. *Neuromethods* 2015; 4: 353–364.
25. Zhou YL, Jiang GQ, Wei J, et al. Enhanced binding capability of nuclear factor-kappaB with demethylated P2X3 receptor gene contributes to cancer pain in rats. *Pain* 2015; 156: 1892–1905.
26. Pan HL, Liu BL, Lin W, et al. Modulation of Nav1.8 by Lysophosphatidic Acid in the Induction of Bone Cancer Pain. *Neurosci Bull* 2016; 32: 445–454.
27. Harms C, Datwyler AL, Wiekhorst F, et al. Certain types of iron oxide nanoparticles are not suited to passively target inflammatory cells that infiltrate the brain in response to stroke. *J Cereb Blood Flow Metab* 2013; 33: 795–796.
28. Hargreaves K. A new and sensitive method for measuring thermal nociception in cutaneous hyperalgesia. *Pain* 1988; 32: 77–88.
29. Galbraith JA, Mrosko B and Myers RR. A system to measure thermal nociception. *J Neurosci Methods* 1993; 49: 63–68.
30. Medhurst SJ, Walker K, Bowes M, et al. A rat model of bone cancer pain. *Pain* 2002; 96: 129–140.
31. Kaan TK, Yip PK, Patel S, et al. Systemic blockade of P2X3 and P2X2/3 receptors attenuates bone cancer pain behaviour in rats. *Brain* 2010; 133: 2549–2564.
32. Coleman JE, Huentelman MJ, Kasparov S, et al. Efficient large-scale production and concentration of HIV-1-based lentiviral vectors for use in vivo. *Physiol Genomics* 2003; 12: 221–228.
33. Xu GY and Huang LY. Peripheral inflammation sensitizes P2X receptor-mediated responses in rat dorsal root ganglion neurons. *J Neurosci* 2002; 22: 93–102.
34. Zhao XH and Zhang T. The up-regulation of spinal Toll-like receptor 4 in rats with inflammatory pain induced by complete Freund's adjuvant. *Brain Res Bull* 2015; 111: 97–103.

35. Yuan B, Tang WH, Lu LJ, et al. TLR4 upregulates CBS expression through NF-kappaB activation in a rat model of irritable bowel syndrome with chronic visceral hypersensitivity. *World J Gastroenterol* 2015; 21: 8615–8628.
36. Planells-Cases R, Garcìa-Sanz N, Morenilla-Palao C, et al. Functional aspects and mechanisms of TRPV1 involvement in neurogenic inflammation that leads to thermal hyperalgesia. *Pflugers Arch* 2005; 451: 151–159.
37. Lingueglia E, Weille JD, Bassilana F, et al. A modulatory subunit of acid sensing ion channels in brain and dorsal root ganglion cells. *J Biol Chem* 1997; 272: 29778–29783.
38. Ogihara Y, Masuda T, Ozaki S, et al. Runx3-regulated expression of two Ntrk3 transcript variants in dorsal root ganglion neurons. *Dev Neurobiol* 2016; 76: 313–322. Doi:10.1002/dneu.22316.
39. Detloff MR, Smith EJ, Quiros Molina D, et al. Acute exercise prevents the development of neuropathic pain and the sprouting of non-peptidergic (GDNF- and artemin-responsive) c-fibers after spinal cord injury. *Exp Neurol* 2014; 255: 38–48.
40. Xu GY, Winston JH, Shenoy M, et al. Enhanced excitability and suppression of A-type K+ current of pancreas-specific afferent neurons in a rat model of chronic pancreatitis. *Am J Physiol Gastrointest Liver Physiol* 2006; 291: G424–G431.
41. Xue ZJ, Shen L, Wang ZY, et al. STAT3 inhibitor WP1066 as a novel therapeutic agent for bCCI neuropathic pain rats. *Brain Res* 2014; 1583: 79–88.
42. Brown R, Imran SA and Wilkinson M. Lipopolysaccharide (LPS) stimulates adipokine and socs3 gene expression in mouse brain and pituitary gland in vivo, and in N-1 hypothalamic neurons in vitro. *J Neuroimmunol* 2009; 209: 96–103.
43. Choi JS, Shin YJ, Cha JH, et al. Induction of suppressor of cytokine signaling-3 in astrocytes of the rat hippocampus following transient forebrain ischemia. *Neurosci Lett* 2008; 441: 323–327.
44. Elsaeidi F, Bemben MA, Zhao XF, et al. Jak/STAT signaling stimulates zebrafish optic nerve regeneration and overcomes the inhibitory actions of socs3 and sfpq. *J Neurosci* 2014; 34: 2632–2644.
45. Fang D, Kong LY, Cai J, et al. Interleukin-6-mediated functional upregulation of TRPV1 receptors in dorsal root ganglion neurons through the activation of JAK/PI3K signaling pathway: roles in the development of bone cancer pain in a rat model. *Pain* 2015; 156: 1124–1144.
46. Camargo CA, Gomes-Marcondes MCC, Wutzki NC, et al. Naringin inhibits tumor growth and reduces interleukin-6 and tumor necrosis factor α levels in rats with Walker 256 carcinosarcoma. *Anticancer Res* 2012; 32: 129–133.
47. Mao-Ying QL, Wang XW, Yang CJ, et al. Robust spinal neuroinflammation mediates mechanical allodynia in Walker 256 induced bone cancer rats. *Mol Brain* 2012; 5: 1–11.
48. Li X, Wang XW, Feng XM, et al. Stage-dependent anti-allodynic effects of intrathecal toll-like receptor 4 antagonists in a rat model of cancer induced bone pain. *J Physiol Sci* 2013; 63: 203–209.
49. Yoshimura A, Naka T and Kubo M. SOCS proteins, cytokine signalling and immune regulation. *Nat Rev Immunol* 2007; 7: 454–465.
50. Qureshi ST, Gros P and Malo D. Host resistance to infection: genetic control of lipopolysaccharide responsiveness by toll-like receptor genes. *Trends Genet* 1999; 15: 291–294.
51. Beutler B. Endotoxin, toll-like receptor 4, and the afferent limb of innate immunity. *Curr Opin Microbiol* 2000; 3: 23–28.
52. Kamizono S, Hanada T, Yasukawa H, et al. The SOCS box of SOCS-1 accelerates ubiquitin-dependent proteolysis of TEL-JAK2. *J Biol Chem* 2001; 276: 12530–12538.
53. Chen JQ, Szodoray P and Zeher M. Toll-like receptor pathways in autoimmune diseases. *Clin Rev Allergy Immunol* 2016; 50: 1–17.
54. Zhang X, Alnaeeli M, Singh B, et al. Involvement of SOCS3 in regulation of CD11c+ dendritic cell-derived osteoclastogenesis and severe alveolar bone loss. *Infect Immun* 2009; 77: 2000–2009.
55. Bai L, Wang X, Li Z, et al. Upregulation of chemokine CXCL12 in the dorsal root ganglia and spinal cord contributes to the development and maintenance of neuropathic pain following spared nerve injury in rats. *Neurosci Bull* 2016; 32: 27–40.
56. Yin Y, Liu W and Dai Y. SOCS3 and its role in associated diseases. *Hum Immunol* 2015; 76: 775–780.
57. Babon JJ, Kershaw NJ, Murphy JM, et al. Suppression of cytokine signaling by SOCS3: characterization of the mode of inhibition and the basis of its specificity. *Immunity* 2012; 36: 239–250.